MICROWAVE EMISSION FROM PULSED, RELATIVISTIC e-BEAM DIODES

I. THE SMOOTH-BORE MAGNETRON

by

T. J. Orzechowski and G. Bekefi

Preprint PFC/JA-78-4

PRR 78/28

Plasma Research Report July 1978

MICROWAVE EMISSION FROM PULSED, RELATIVISTIC e-BEAM DIODES*

I. THE SMOOTH-BORE MAGNETRON

by

T. J. Orzechowski† and G. Bekefi

Department of Physics and Research Laboratory of Electronics
Massachusetts Institute of Technology
Cambridge, Massachusetts 02139

Abstract

We report measurements of intense magnetron oscillations in pulsed, field-emission diodes (~350 kV, 30 nsec) subjected to crossed externally applied magnetic fields ($\lesssim$16 kG). The oscillations set in as soon as the magnetic field exceeds the critical field necessary for cutting off the diode current. The oscillations are diagnosed by the microwave emission which is studied in the range from 7 to 40 GHz. The radiation is emitted in broad frequency bands, it is strongly polarized, and can be tuned by the magnetic field; the power levels are typically 1 to 5kW. The observations are consistent with the onset of the slipping stream instability in the Brillouin space charge flow of the electron cloud.

---

*This work was supported in part by the Air Force Office of Scientific Research (Grant AFOSR77-3143), and in part by the United States Department of Energy (Contract EY76-S-02-2766).

†Present address: Lawrence Livermore Laboratory, Livermore, California

1. INTRODUCTION

The smooth-bore magnetron diode comprises a cylindrical anode of radius r_a enclosing a coaxial cylindrical cathode of radius r_c as is illustrated in Fig. 1. The electrons emitted by the cathode are subjected simultaneously to two steady, or quasi-steady fields acting at right angles to one another: a uniform, axial magnetic field B_z produced by, say, a solenoid, and a radial electric field $E_r(r)$ generated by applying voltage V between the two electrodes.

In conventional magnetron diodes[1-3] voltages of a few volts to several kilovolts are applied between the anode and a thermionically emitting cathode. Typical currents that can be furnished by the cathode range from milliamperes to a few tens of amperes. This article is concerned with a magnetron diode having the conventional geometry described above. However, it differs in that the electrons are generated by field emission from a cold graphite cathode, and currents of 50 to 100 kA can thus be drawn across millimeter wide vacuum gaps. The applied voltages of 200-400 kV are pulsed and have a duration of 30 nsec. As is described in detail elsewhere[4,5] the requisite power is generated by the high voltage facility "NEREUS" capable of supplying 1.3kJ of beam energy at 600 kV to a matched 4 ohm load.

We note that in order to obtain significant field emission the anode-cathode gap $d=(r_a-r_c)$ is necessarily small. This has the consequence that in our studies the quantity $(r_a-r_c)/r_a$ is much less than unity (it lies typically in the range from 0.1 to 0.2) and the geometry approaches that of the so-called[6] "planar magnetron" diode. On the other hand, conventional low voltage, low current diodes operate in the regime $0.5 \lesssim (r_a-r_c)/r_a \lesssim 1$.

In this paper we shall be concerned with magnetron oscillations which set in as soon as the magentron field B_z exceeds a critical field B* char-

acterized by the requirement that the gyro-radius of an electron emitted from the cathode equals the gap width $d = (r_a - r_c)$. This "Hull cutoff" condition[7] is given by the formula

$$B^* = (m_o c/ed_e)[\gamma_o^2 - 1]^{1/2} \quad \text{Tesla} \quad (1)$$

with

$$\gamma_o \equiv 1 + (eV/m_o c^2)$$

where V is the voltage across the gap $d = r_a - r_c$, e and m_o are the electron charge and rest mass, respectively, and $d_e = (r_a^2 - r_c^2)/2r_a$ is the effective gap width. We note that Eq. (1) can be derived from a single particle calculation;[7,8] however, it is also obtained from a fully relativistic magnetohydrodynamic computation which allows for electric space charge and self-magnetic fields of the electron cloud.[9] Figure 2 illustrates that a sharp cutoff at $B_z = B^*$ is indeed achieved in our field-emission, relativistic electron beam diodes.

In the regime of magnetic fields defined by $B_z < B^*$ the current-voltage characteristics of the diode are well represented[4] by the Child-Langmuir space charge limited flow $I_{CL} \propto V^{3/2}/d^2$ modified[10] by two effects. The first is caused by the fact that the electron trajectories are curved by the magnetic field B_z which raises their transit time. The Child-Langmuir current then falls slightly as B_z is increased from zero towards B*, because the "slowed" electrons provide increased space charge shielding near the cathode against the anode potential. However, a more important departure from conventional Child-Langmuir operation in our large current diodes is caused by the strong azimuthal self-magnetic field $B_\theta = \mu_o I_z/2\pi r$ generated by axial current I_z flowing along the cathode and the steel shank which attaches the latter electrode to the NEREUS generator (this effect is negligible in conventional diodes where I_z is small).

Approximate calculations[5] show that now the current flowing across the gap is given by

$$I \simeq \frac{2\pi r_a B^*}{\mu_o}\left[1 - \left(\frac{B_z}{B^*}\right)^2\right]^{1/2} \qquad B_z < B^*$$
$$= 0 \qquad B_z > B^* \tag{2}$$

a result which is compared with measurements in Fig. 3. It is seen that the experiments are in quite satisfactory agreement with calculations for the regime $B_z < B^*$. However, there are serious discrepancies for $B_z > B^*$, where small but by no means negligible flows of current across the gap persist (typically 2 to 5% of maximum current). This fact is clearly seen in Fig. 4 in which we plot on a linear scale the diode current and voltage as a function of magnetic field, for fields both smaller and larger than B*. Even when B_z is twice as great as B*, approximately 1kA of current flows. It may be thought that because of end effects (the electrodes are after all of finite length), magnetic field inhomogeneity, and misalignments of the diode, some electrons may flow along the magnetic field lines and be collected. To ensure that none of these currents are received by our measuring probe, and that I is indeed the radially flowing current, shields[5] are provided to protect the current measuring probe from the unwanted signals.

It is appropriate at this point to note the meaning of the Hull cutoff condition given by Eq. (1). It states that subject to the assumption of zero initial electron velocities and no time variation in any field quantities, there can be no current to the anode if the magnetic field is greater than the cutoff field B*. This is independent[8] of the degree of space charge at the cathode or, for that matter, the detailed nature of the steady space-charge state. Thus, ideally, the diode is "magnetically insulated."

Under conditions of perfect magnetic insulation, (if this state were ever to exist) a steady state can occur in which the electrons within the space charge cloud follow paths which are independent of time. The actual form of the steady state has been the subject of much investigation. In general the state is not unique because one must make assumptions about the initial electron distribution in the space charge cloud. There are two classes of solution that have attracted the most attention. They are (a) the "double-stream" state in which the electrons make cycloidal orbits which commence and finish on the cathode surface;[11-18] and (b) the "single-stream" state[19-23] in which the electrons move parallel to the electrode surfaces, with drift velocities given by $\vec{v} = \vec{E}\times\vec{B}/|B|^2$. The electron motion corresponding to this state is also known as "Brillouin flow" or "parapotential flow,"[19,21] the latter signifying that the electrons move along equipotentials rather than along field lines, as is customary. In this model the space charge extends from the cathode $r=r_c$ to some radius $r=r_o$ but there are no electrons within the space between $r=r_o$ and the surface of the anode at $r=r_a$. The thickness of the space charge cloud (r_o-r_c) is a function of magnetic field, and varies approximately as $(B^*/B_z)^2$. The space charge drift speed $v_\theta=E_r/B_z$ is strongly sheared: it is zero at the cathode surface $r=r_c$ and rises rapidly with r, reaching maximum velocity at the surface of the space charge cloud at $r=r_o$. The velocity of the surface layer has been calculated for the case of the "planar magnetron diode" (that is for $(r_a-r_c)/r_a<<1$) and the results of the calculations are shown in Fig. 5. We see that velocities of relativistic magnitudes are readily achieved in our type of field emission diodes. And, whereas, no current flow to the anode can occur, there is a large <u>circulating</u> current in the azimuthal direction. At $B_z=B^*$, the magnitude of this "Brillouin" current is given by[22]

$$I_\theta = (m_o c/ed)(L/\mu_o)(\gamma_o - 1)\cosh(\gamma_o) \text{ Amp.} \quad (3)$$

where $\gamma_o \equiv 1 + (eV/m_o c^2)$ and L is the length of the cathode as measured along the z axis. As B_z increases, I_θ falls because the space charge cloud becomes thinner. This variation with B_z is shown plotted in Fig. 6.

The opinion is that Brillouin flow is the more likely state into which the system will settle initially provided that the risetime of the voltage pulse is slow compared with the cyclotron period, so that adiabaticity can be invoked in the equations of motion. This view is reinforced by computer calculations[24] of the electron trajectories showing the unmistakable evolution of the Brillouin state. Furthermore, it was proved,[25] for nonrelativistic cylindrical diodes at least, that the Brillouin single stream state is the only one possible whenever $r_o/r_c < R \approx 2$ where r_c is the radius of the cathode and r_o is the radius of the outer boundary of the space charge cloud. The parameter R is approximately equal to 2, but its magnitude varies somewhat with the value of the current associated with the Brillouin $\vec{E}\times\vec{B}$ flow. The above inequality is well satisfied in all our experiments where $1<R<1.2$.

It is generally accepted that a manifestation of currest flow across the vacuum gap is due to a breakdown of the steady state assumption; namely, time varying, organized, electric and magnetic field oscillations (i.e. instabilities) develop resulting in the destruction of the steady state flow and creation of large amplitude electromagnetic oscillations. And, it is these oscillations that are the subject matter of section 3 below. It is worth noting that the degree of organization of the oscillatory fields is greatly enhanced by piercing the anode with a chain of coupled cavity resonators, a procedure one adopts in the practical magnetron devices. This will be the subject of a subsequent paper (II) (see also ref. 26) where we

shall show that, using our relativistic electron, field-emission cathode, microwave oscillations in the gigawatt range of powers can be achieved.

2. THE EXPERIMENTAL ARRANGEMENT

The outer stainless steel anode is a cylinder 4.4 cm in diameter and 4.0 cm long.[4,5] It is polished and has rounded edges to minimize local field enhancement and arcing. The inner coaxial cathode is machined from dense, fine-grained graphite. A number of cathodes with diameters varying between 3.36 cm to 3.98 cm is used, thus providing diodes having gaps with spacings d ranging from 2.3 mm to 5.4 mm. The cathode is connected via a stainless steel shank to the inner conductor of the water filled coaxial capacitor which serves as the transmission line of the 4 ohm NEREUS high voltage facility. The anode is connected via a shielded current viewing probe (see above) to the outer, grounded wall of the capacitor. The system is continuously pumped by means of a diffusion pump to pressures of approximately 5×10^{-5} Torr.

The axial magnetic field B_z acting on the diode is generated in a solenoid energized by a capacitor bank whose rise time is approximately 6 msec. The discharging of this bank is timed in such a way that B_z reaches its peak value when NEREUS fires. Thus, the magnetic field is virtually constant in time over the duration of the 30 nsec voltage pulse applied across the diode. The thin-walled, stainless steel construction of the diode ensures good penetration of the pulsed magnetic field into the diode interior. A magnetic field as high as 16 kG can be generated.

The diode current is measured with a rapidly responding, low-inductance current viewing probe; its output is displayed on a fast oscilloscope. The diode voltage is obtained from the signal delivered by a calibrated copper-sulphate voltage divider network and is corrected for inductance effects.[4,5]

The magnetron oscillations are diagnosed by monitoring the microwave radiation emitted by the diode in an arrangement illustrated schematically in Fig. 7. The waves emanate from the diode via a low loss polystyrene window and are received by a microwave horn. The received power is first attenuated to suitable levels by means of a precision attenuator and then measured with a calibrated crystal detector connected to a fast oscilloscope. Thus, the power $P_r(R,\theta,\phi)$ received at a given point in space distant R from the diode, and at an angular position (θ,ϕ) with respect to the diode axis is found with good accuracy. The distance R is sufficiently large so as to ensure that the transmitting magnetron diode and the receiving horn are in each others radiation fields; that is $R \gtrsim 2D^2/\lambda$ where D is the characteristic size of the transmitter or receiver, whichever is the larger, and λ is the wavelength. With this choice of R, the power P_e emitted by the magnetron diode is related to the power received P_r, through the well-known radar formula[27]

$$P_e = P_r[16\pi^2 R^2/G_e G_r \lambda^2] \tag{4}$$

where G_e is the gain of the transmitting diode and G_r the gain of the receiving horn. The receiving antenna is a standard horn and its gain G_r is known. The gain of the emitter G_e is obtained by making an angular scan of the transmitted power, and then deriving G_e from the relationship[27]

$$G_e = \frac{4\pi P_r(\theta,\phi)}{\int P_r(\theta,\phi)\sin\theta \, d\theta d\phi} \tag{5}$$

Using the measured values of $P_r(\theta,\phi)$, allows one to carry out numerically the integration demanded in the denominator of Eq. (5).

From the foregoing procedure, the power emitted by the magnetron diode is determined. The measurements are made over frequencies ranging from 7 to 40 GHz with suitable microwave plumbing used for each of the

four frequency bands needed to explore this large range: X-band (7-12.4 GHz), K_u band (12.4-18 GHz), K band (18-26.5 GHz) and K_a band (26.5-40 GHz). No measurements were attempted at lower frequencies because the outer cylindrical anode acts as a waveguide beyond cutoff. It cuts off the lowest TE_{11} mode at 4 GHz and the TE_{01} mode of interest here (see below) at 8.3 GHz. The X-band receiver cuts off at 7.2 GHz.

The spectral distribution of the emitted radiation is determined by interposing a length ℓ of dispersive line between the receiving horn and the crystal detector. The time delay t suffered by the signal relative to the time (t=0) of the arrival of undispersed signal (see Fig. 7) allows one to decompose the measurements into the various frequency components, using the relationship that $\ell = v_g(\omega)t$, where $v_g(\omega)$ is the group velocity. The group velocity is obtained from knowledge of the dispersion characteristics of the waveguide used in our experiments with the result that the frequency ω of the dispersed signal is given in terms of the waveguide cutoff frequency ω_c by

$$\omega=\omega_c[1 - (\ell/ct)^2]^{-1/2} \qquad (6)$$

We use 155 meters of waveguide. Since only X-band waveguide of such lengths is available to us, all our spectral frequency measurements are made in the regime from ~7 to ~12 GHz.

3. MEASUREMENTS

The measurements fall into three categories. A study of the rf emission as a function of the externally applied magnetic field B_z; determination of the frequency characteristics; and a determination of the rf electric field configuration, namely its polarization. We begin with a discussion of the magnetic field dependence.

(a) Magnetic Field Characteristics of the Emitted Radiation

In our experiments we adopt the following procedure. We arrange the microwave instrumentation for the desired band (X, K_u, K, K_a). We set the externally applied magnetic field B_z to a given value and charge NEREUS to a fixed constant voltage. We then measure the total microwave power P_r received by a small horn placed in the radiation zone of the transmitting diode (Fig. 7), together with the diode current I and the diode voltage V. With the same charging voltage we change the magnetic field to a new value and repeat the measurements of P_r, I and V. Note that although the charging voltage is maintained the same throughout a run, the voltage V across the magnetron diode varies somewhat with changing B_z (see Fig. 4) because of changes in the diode impedance.

A series of successive shots like those described are then assembled to yield P_r as a function magnetic field, at roughly constant diode voltage. The measurements are then repeated for all the remaining microwave bands.

By scanning the magnetic field from $B_z \simeq 0$ to $B_z \simeq 16$ kG we verify that within the sensitivity of our microwave detection system, no significant radiation occurs at any frequency until the magnetic field is close to, or exceeds, the critical field B*. A further increase in the magnetic field causes the emission to rise sharply, reach a peak value at some value $B_z = B_z(\max)$, and then fall rapidly. This "resonant" behavior is illustrated in Fig. 8 which shows plots of the radiation intensity in two different frequency bands (X and K_a) as a function of B_z. Measurements made in other frequency bands show similar characteristics. These can be summarized as follows. First, the radiation sets in at a certain value of B_z near $B_z = B^*$ and the onset is the same at all frequencies. Secondly, the peak in the microwave radiation occurs at a definite value

of the applied magnetic field $B_z = B_z(max)$: the value of $B_z(max)$ is different depending on the frequency band under investigation, as is clearly seen from Fig. 8. Thirdly, the total power outputs P_e (obtained from radiation pattern measurements and use of Eqs. 4 and 5) are approximately the same in all four frequency bands examined. Figure 9 illustrates both the power and the tuning characteristics of the diode. In each of the four microwave bands the total emitted power is typically 1 to 5 kW. And, the higher the externally applied magnetic field, the higher is the frequency of the microwaves received. The "tuning" relationship is approximately linear and is of the form

$$f \simeq 3{\cdot}4\times10^{9}(B_z - B^*) \quad \text{Hz} \tag{7}$$

where B is in kG.

(b) Frequency Characteristics

The shape of the curves shown in Fig. 8 and the tuning characteristics illustrated in Fig. 9 point to the fact that we are dealing here with multiple resonance behavior. Spectral measurements in which we observe one, two, and even several resonances bear this out. The measurements are carried out (for fixed B_z and diode voltage V) by means of the dispersive line described in Section 2. Figure 10 is typical of such observations. It shows that at a given magnetic field (which we have chosen in the figure to be that corresponding to maximum emission at X-band) there are two fairly wide ($\lesssim$1 GHz) resonances. As the magnetic field is varied, the frequency positions of the resonances and their separation remain unchanged even when the magnetic field is varied by as much as a factor of two. However, their amplitudes vary strongly with B_z and reach maximum values only for a certain fixed $B_z = B_z(max)$. New resonances may appear at widely different magnetic fields but usually there is only one very strong resonance flanked by one or more rather weak ones.

Are the above resonances inherent to the emission process of the radiating electrons such as cyclotron or plasma oscillations, and are they therefore governed by the dispersion characteristics of the electron gas? The answer is no. The resonances are system resonances that are there even in the absence of the electrons. This has been verified in "cold tests" of the diode. A low level microwave signal of variable frequency is injected into the diode and a small probing antenna measures the response. One then finds resonances having identical frequencies and Q's as in the operating diode. A second test is used to verify that the resonances are simply system resonances of what is after all a fairly complicated cylindrical resonant cavity. We vary the gap width d and find no change in the emission spectrum, despite the fact that the Brillouin space charge flow is a sensitive function of d.

Thus, the following picture emerges concerning the spectral characteristics of the radiation. Copious emission, exceeding expected thermal levels by many orders in magnitude, is generated by the rotating electron space charge cloud. The cloud is unstable resulting in the production of intense rf electric field fluctuations which exist over a fairly broad frequency spectrum. As a result of system resonances, the electromagnetic radiation ultimately emanating from the diode is enhanced at those particular frequencies which correspond to certain resonant frequencies of the "cold" resonator system. In other words, the emission "locks onto" one or another of the many possible cavity modes. The resonances can be tuned with magnetic field and are observed in one of two ways: from the frequency spectrum, at constant B_z (Fig. 10); or by sweeping B_z, keeping the observation frequency fixed constant over the discrete frequency bands, X, K_u, K, K_a (Figs. 8 and 9).

(c) Polarization

The radiation emanating from the polystyrene window is strongly polarized, with electric field lines forming predominantly concentric circles about the diode axis. This is verified by placing two receiving horns in the radiation zone at fixed and equal distances R from the diode and scanning in angles θ or ϕ. The horns are rotated at right angles to one another and are thus sensitive to orthogonal electric field polarizations. In addition to the strongly polarized field, there is evidence of a weak background of randomly polarized radiation.

The strongly polarized component is consistent with the emission from a circular waveguide excited in the TE_{01} mode (or possibly in a higher TE_{0m} mode). The accompanying radiation pattern obtained by sweeping the angle θ at constant R and ϕ is illustrated in Fig. 11 for K_a band frequencies. The "butterfly shaped" pattern with two well-pronounced wings, and a minimum in intensity at $\theta=\phi=0$ is typical[28] of the TE_{01} mode of excitation. (The same type of radiation pattern is also seen at X, K_u, and K band frequencies.) As additional verification, we point out that no emission from the diode is ever observed at a frequency below approximately 8.2 GHz (see Fig. 10). Now, the cutoff frequency of a cyclindrical waveguide oscillating in the TE_{01} mode is given by $f_c = 0.610(c/a)$ where a is the radius. With a = 2.22cm, f_c = 8.3 GHz, a result which is in good agreement with observations. We note in passing that the TE_{01} mode is not the lowest (or fundamental) mode of a circular pipe. The lowest mode is the TE_{11} mode which has a cutoff frequency (for our radius of pipe) equal to 4.0 GHz.

4. DISCUSSION

The intensity of the rf electric field fluctuations associated with

observed microwave power output must, indeed, be quite substantial. Take a power output of 5kW and assume a 10 percent efficiency of converting electromagnetic energy within the 3.4mm cathode-anode gap into transverse electromagnetic wave energy outside the diode. It then follows from Poynting's flux that the peak electric fields in the gap are typically 9 kV/cm, or approximately equal to 1 percent of the dc radial electric field applied across the anode-cathode gap. This agrees with earlier estimates made for conventional magnetrons in which fluctuations as high as 10 percent of the dc value have been reported.[29]

That fluctuations set in at the critical magnetic field $B_z=B^*$ points to the fact that the instability is associated with the Brillouin space charge flow which sets in precisely at this critical field. As noted in Section 1, the azimuthal flow is sheared which can result in the so-called slipping stream[30] or diochotron instability. It is a space charge instability in which the surface of the Brillouin cloud becomes rippled in the azimuth; associated with this rippling is an azimuthal rf electric field. This field has the correct polarization to excite a TE_{0m} mode in the circular diode. The fact that the observed emission is principally in the TE_{01} mode lends credence to our belief that we are in fact dealing here with a manifestation of the slipping stream instability. In particular, we think that it is a slipping stream mode effected by resistive wall effects.[30] The latter makes the instability "go" at frequencies less than the cyclotron frequency, as observed by us. To verify this, however, would require a measurement of the wavelength of the instability and comparison with the theoretically predicted dispersion equation. Unfortunately, the measurement of the wavelength of the space charge fluctuations is difficult if not impossible in our pulsed diode.

Other instabilities come to mind, particularly those at frequencies

corresponding to the electron-cyclotron and electron-plasma frequencies. The first can be ruled out on the grounds that all our measurements show (Fig. 9) that the emission is broad band and occurs well-below the relativistic cyclotron frequency $\omega_c = eB/m\gamma$. The second is ruled out for the same reason, since for space charge limited flow, the plasma frequency ω_p equals the cyclotron frequency ω_c.

The presence of ions (due to anode and/or cathode plasma formation) can lead to ion type of instabilities which have sometimes been seen[31] in conventional magnetrons. However, these instabilities result in low frequency fluctuations in the range of tens of megahertz. If they are present in our diode, they could not be observed by our measureing technique.

In conclusion, then, we have shown that a strong correlation exists between the observed anomalous current flow across the relativistic magnetron diode when $B_z > B^*$, and the intense microwave emission emanating from it. We believe that the origin of the emission is a form of the slipping instability in the Brillouin space charge flow. A full electromagnetic and relativistic r,θ particle simulation code is under development with whose aid we hope to be able to answer this question.[32] In particular, we expect that the code will yield information about the dependence of the diode current on magnetic field (see Fig. 4), a problem that has so far defied detailed theoretical understanding (but see Mouthaan and Süsskind of Ref. 30). Needless to say, the smooth-bore magnetron has little or no application as a device for generating microwaves. It has poor efficiency, and the emission spectrum is broad and not readily controlled. But, it is, so to speak, the basic building block of real magnetron devices which differ from the smooth-bore in that the anode block is pierced by a series of coupled resonators. The oscillations seen in the smooth-bore diode are believed to come close to the startup

conditions of the real device. Thus, in the initial state (often referred to as the "preoscillation stage") the interaction is predominantly quasi-electrostatic in character: the electrons interact collectively with longitudinal space charge electric fields generated in the bulk and near the surface of the space charge cloud. The associated Poynting flux is relatively small. This differs from the fully developed oscillating stage of the magnetron device which is characterized by strong energy exchange between the electrons and the transverse electromagnetic fields which exist outside the main space-charge cloud, that is, between the anode and the space charge boundary. The strong interaction is the consequence of electromagnetic modes that are in phase synchronism with the rotating Brillouin cloud. Now the Poynting flux becomes enormous, but this is the subject matter of a subsequent report (paper II).

REFERENCES

1. J. A. Bradshaw, article in "Crossed-Field Microwave Devices", E. Okress, editor (Academic Press 1961) Vol. 1, p. 261, plus references in this article.

2. J. M. Osepchuk, article in "Crossed-Field Microwave Devices", E. Okress, editor (Academic Press 1961) Vol. 1, p. 275, plus references in this article.

3. G. D. Sims, article in "Crossed-Field Microwave Devices", E. Okress, editor (Academic Press 1961) Vol. 1, p. 179.

4. T. J. Orzechowski and G. Bekefi, Phys. Fluids 43, 19, (1976).

5. G. Bekefi, T. J. Orzechowski, and K. D. Bergeron, First International Topical Conference on Electron Beam Research and Technology, Albuquerque, 1975, National Technical Information Service, U.S. Department of Commerce Vol. I, p. 303, 1976.

6. O. Buneman, Nature 165, 474 (1950).

7. A. W. Hull, Phys. Rev. 18, 31 (1921).

8. L. Page, Phys. Rev. 18, 58 (1921).

9. R. V. Lovelace and E. Ott, Phys. Fluids 17, 1263 (1974).

10. L. Tonks, Phys. Sowjetunion 8, 572 (1936); K. D. Bergeron and J. W. Poukey, Appl. Phys. Letters 27, 58 (1975).

11. D. R. Hartree, C.V.D. Rept. Mag. 1 (1941).

12. J. Slater, "Microwave Electronics", Van Nostrand 1950.

13. J. L. Delcroix, Thesis, Paris University 1953 (unpublished).

14. D. Gabor, Proc. Roy. Soc. A,183, 436 (1945),; D. Gabor and G. D. Sims, J. Electronics 1, 25 (1955).

15. R. Q. Twiss, Advances in Electronics 5, 247, (1953); J. Electronics 1, 1 (1955).

16. R. N. Sudan and R. V. Lovelace, Phys. Rev. Letters 31, 1174 (1973).

17. R. V. Lovelace and E. Ott, Phys. Fluids 17, 1263 (1974).

18. A. Ron, A. A. Mondelli, and N. Rostoker, IEEE Trans. Plasma Sci. PS-1, 85 (1973).

19. L. Brillouin, Phys. Rev. 60, 385 (1941); 62, 166 (1942); 63, 127 (1943); L. Brillouin, and F. Block, Advances in Electronics 3, 85 (1951); 3, 145 (1951).

20. O. Buneman, Nature 165, 474 (1950); J. Electronics and Control 3, 1 (1957); 3, 507 (1957); C.V.D. Rept. Mag. 10, 11, 17, 30. (1943).

21. B. C. DePackh, Naval Research Laboratory Radiation Project Progress Report No. 5 (1968); 17 (1969). (Unpublished).

22. E. Ott and R. V. Lovelace, Appl. Phys. Letters 27, 378 (1975).

23. J. M. Creedon, J. Appl. Phys. 46, 2946 (1975); 48, 1070 (1977); S. A. Goldstein, R. C. Davidson, J. G. Siambis and R. Lee, Phys. Rev. Letters, 33, 1471 (1974).

24. O. Buneman, article in "Crossed-Field Microwave Devices", E. Okress, editor (Academic Press, 1961) Vol. 1 p. 209.

25. W. P. Allis, M.I.T. Radiation Laboratory Report No. V-9,S, Oct. 1941.

26. G. Bekefi and T. J. Orzechowski, Phys. Rev. Letters, 37, 379 (1976).

27. S. Silver, "Microwave Antenna Theory and Design", M.I.T. Radiation Laboratory Series Vol. 12 (McGraw-Hill, 1949) p. 4.

28. N. Marcuvitz, "Waveguide Handbook", M.I.T. Radiation Laboratory Series Vol. 10 (Boston Technical Publishers, Inc., 1964) p. 201.

29. C. W. Hartman, Electronics Research Laboratory Report No. 10, 1960, University of California, Berkeley, California.

30. O. Buneman, article in "Crossed-Field Microwave Devices", E. Okress

editor (Academic Press 1961) Vol. 1, p. 367; G. G. Macfarlane and H. G. Hay, Proc. Phys. Soc. 63, 409 (1950); K. Mouthaan and C. Süsskind, J. Appl. Phys. 37, 2598 (1966); O. Buneman, R. H. Levy and L. M. Linson, J. Appl. Phys. 37, 3203 (1966).

31. V. I. Farenik, V. V. Vlasov, A. M. Rozhkov, K. N. Stepanov, and V. A. Suprunenko, Zh. Tekh. Fiz. 42, 1625 (1972) [Sov. Phys. Tech. Phys. 17, 1298 (1973)]; also Zh. Eksp. Teor. Fiz Pis. Red. 10, 71 (1969) [J.E.T.P. Lett. 10, 46 (1969)].

32. An early attempt at this was made by S. P. Yu, G. P. Kooyers and O. Buneman, J. Appl. Phys. 36, 2550 (1965).

FIGURE CAPTIONS

Fig. 1. Geometry of the smooth-bore magnetron.

Fig. 2. Diode perveance as a function of the normalized magnetic field B_z/B^*, for different gap widths d. The perveance is determined at a time during the 30 nsec pulse when maximum current is drawn to the anode. The curves for the different gap widths are displaced vertically with respect to one another by a fixed interval, for easier visual presentation. Absolute magnitudes of the perveance, at $B_z=0$, for each of the four gaps, are respectively: 1052 (1149); 589 (522); 329 (310); 202 (205) $\mu AV^{-3/2}$, where the values in parentheses are from the Child-Langmuir theory.

Fig. 3. Normalized electron current I/I_L as a function of the normalized magnetic field B_z/B^*. I_{CL} is the Child-Langmuir current in the limit, $B_z \to 0$. The "hot tial" at $B_z > B^*$ has been omitted from this figure for the sake of clarity. The various points are experimental values obtained for different gap widths: O O, d = 2.3 mm; ● ●, d = 3.4 mm; X X, d = 4.4 mm; Δ Δ, d = 5.4 mm. The solid line is from theory[5,10] for a planar diode in a uniform magnetic field. The dashed curve is from Eq. (2).

Fig. 4. Diode current and diode voltage as a function of magnetic field, for a gap width d = 3.4 mm. The current (and voltage) are measured at a time during the pulse corresponding to maximum current flow. The critical magnetic field B* = 5.5 kG.

Fig. 5. Brillouin drift velocity of the outermost space charge layer of a planar diode, as a function of magneitc field, calculated for different diode voltages V.

Fig. 6. The azimuthal Brillouin current calculated in the limit $(r_a-r_c)/r_a \ll 1$ of a plasma magentron diode, as a function of magnetic field. The value of current at $B_z=B^*$ shown by the heavy dot is given by Eq. 3. Only part of this current appears across the diode when magnetic insulation breaks down, but precisely what fraction depends on the spectrum and amplitude of the turbulent rf fields, and is a largely unsolved problem (but see Mouthaan and Süsskind of Ref. 30).

Fig. 7. Experimental arrangement used in studying microwave emission from the diode.

Fig. 8. Total microwave power emitted in two frequency bands, as a function of magnetic field; d = 3.4mm.

Fig. 9. Frequency and power of emitted radiation as a function of magnetic field. In each frequency band the magnetic field $B_z = B_z(\max)$ is adjusted to give maximum power output (see Fig. 8).

Fig. 10. Spectrum of emitted radiation in the X-band range of frequencies; f_c is the cutoff frequency of the TE_{01} mode.

Fig. 11. Observed radiation pattern (i.e. a polar plot of intensity as a function of angle θ) in the K_a band range of frequencies (26-40 GHz). The fact that the intensity does not go exactly to zero on axis ($\theta=90°$) is partly due to the finite size of the receiving horn and partly due to the presence of a weak component of randomly polarized radiation.

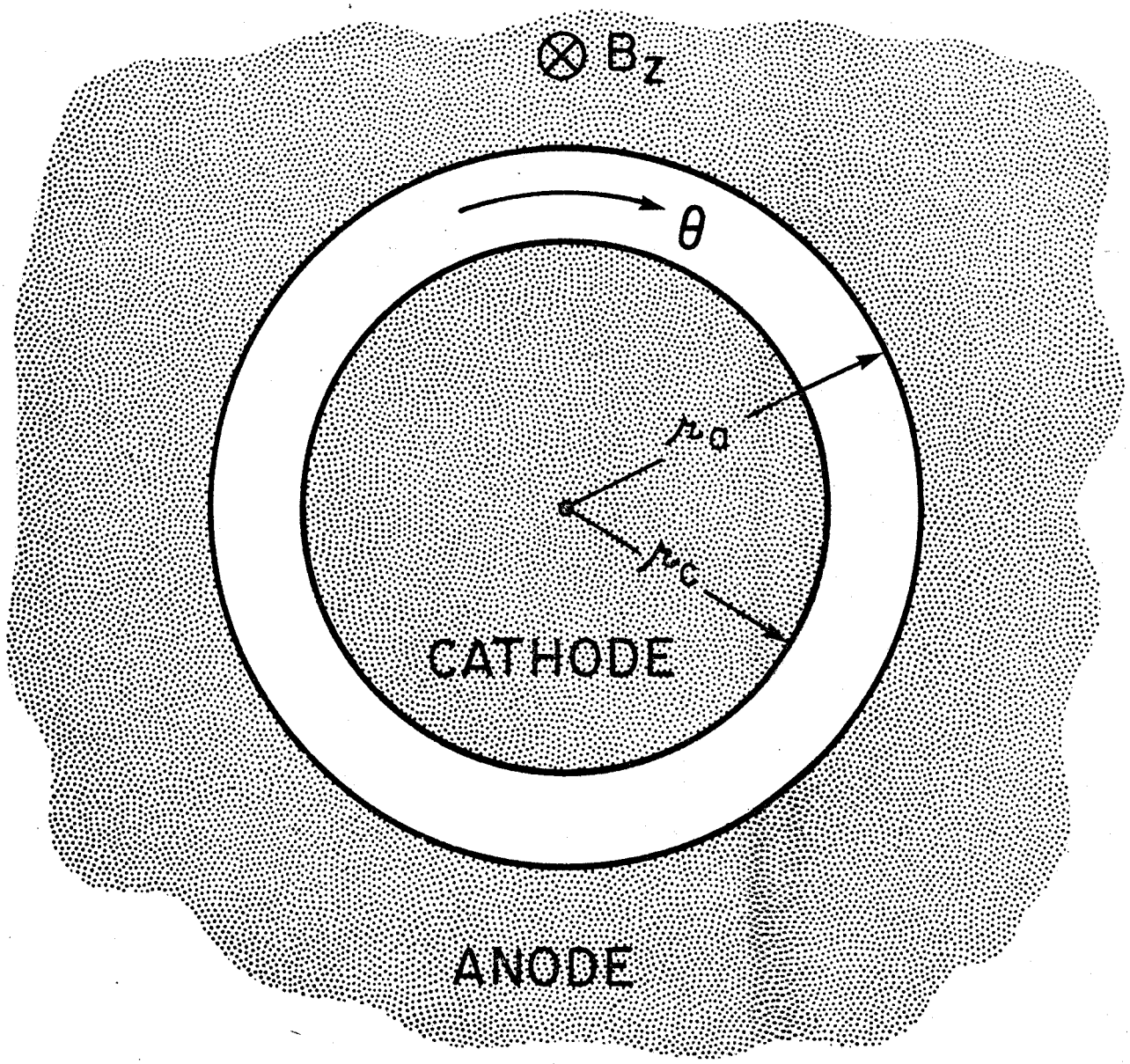

Fig. 1
Orzechowski & Bekefi

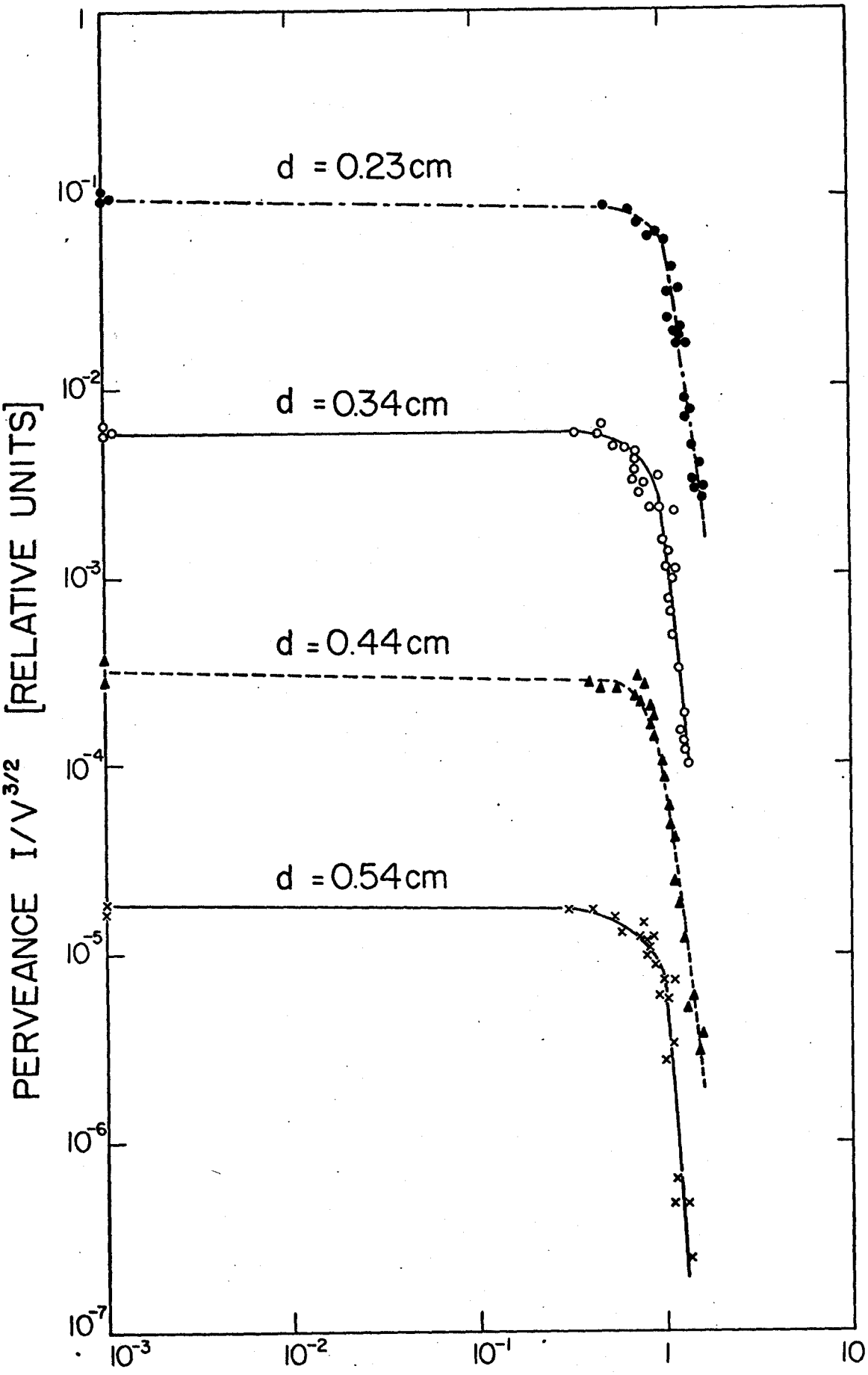

Fig. 2
Orzechowski & Bekefi

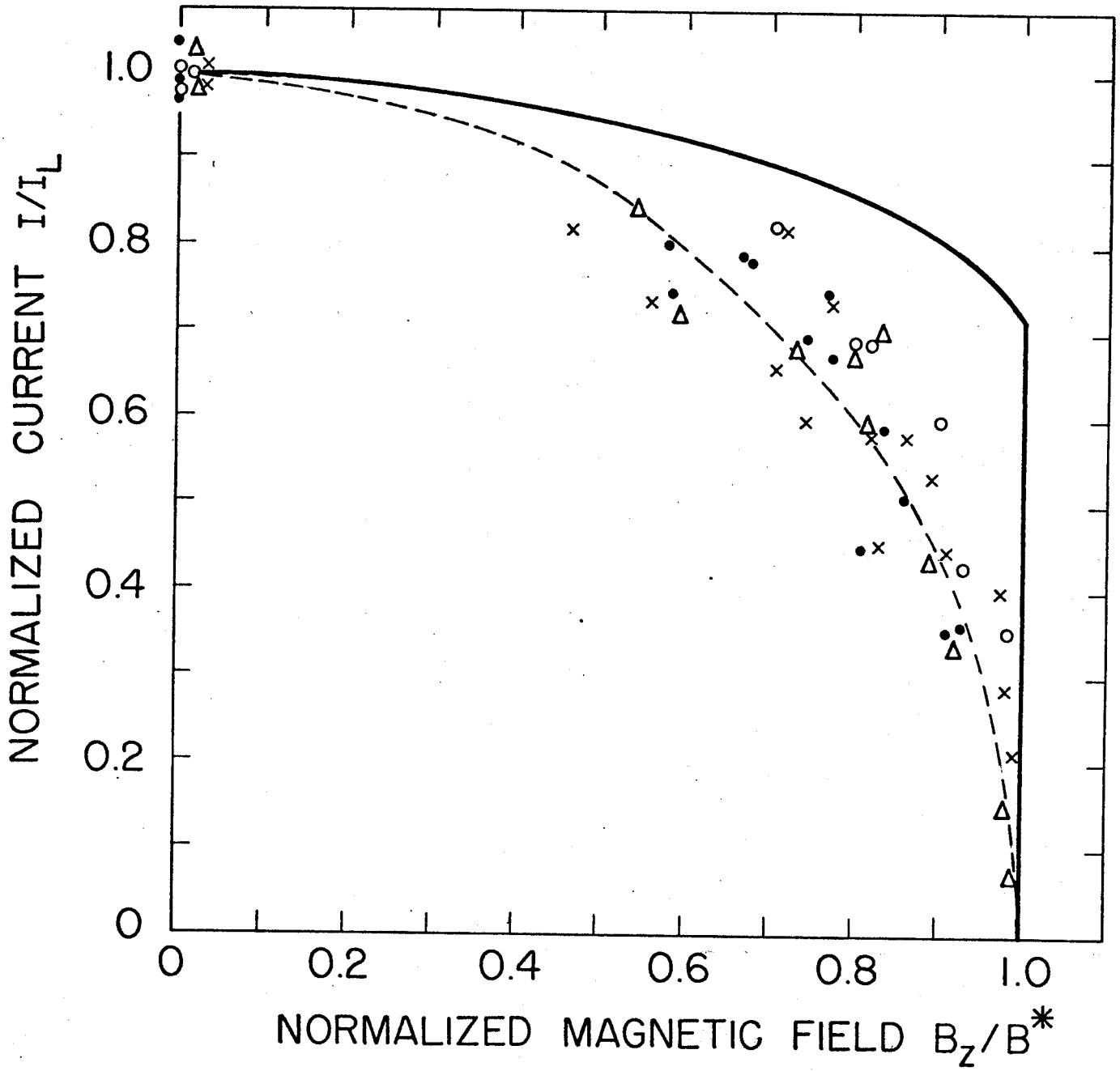

Fig. 3
Orzechowski & Bekofi

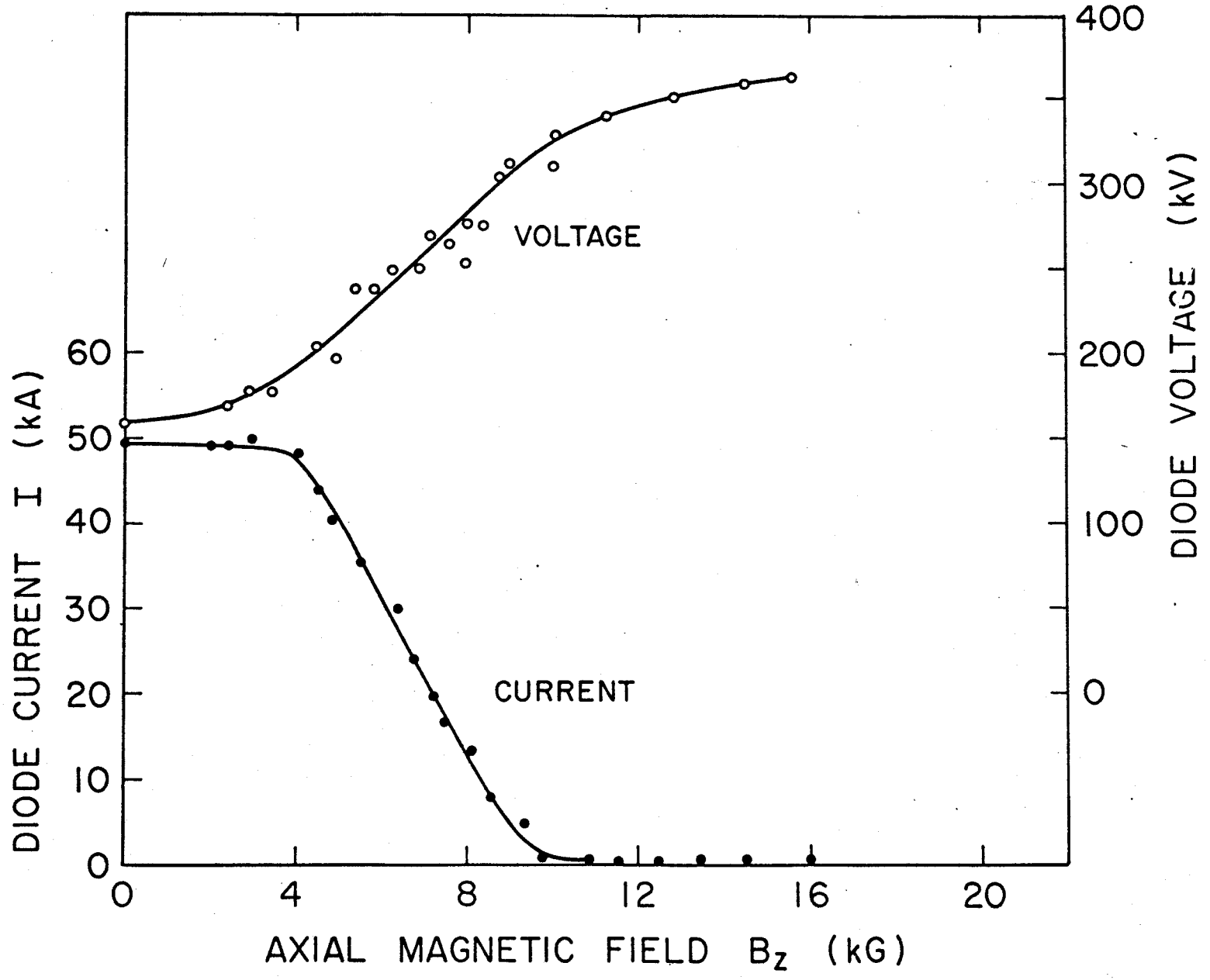

Fig. 4
Orzechowski & Bekefi

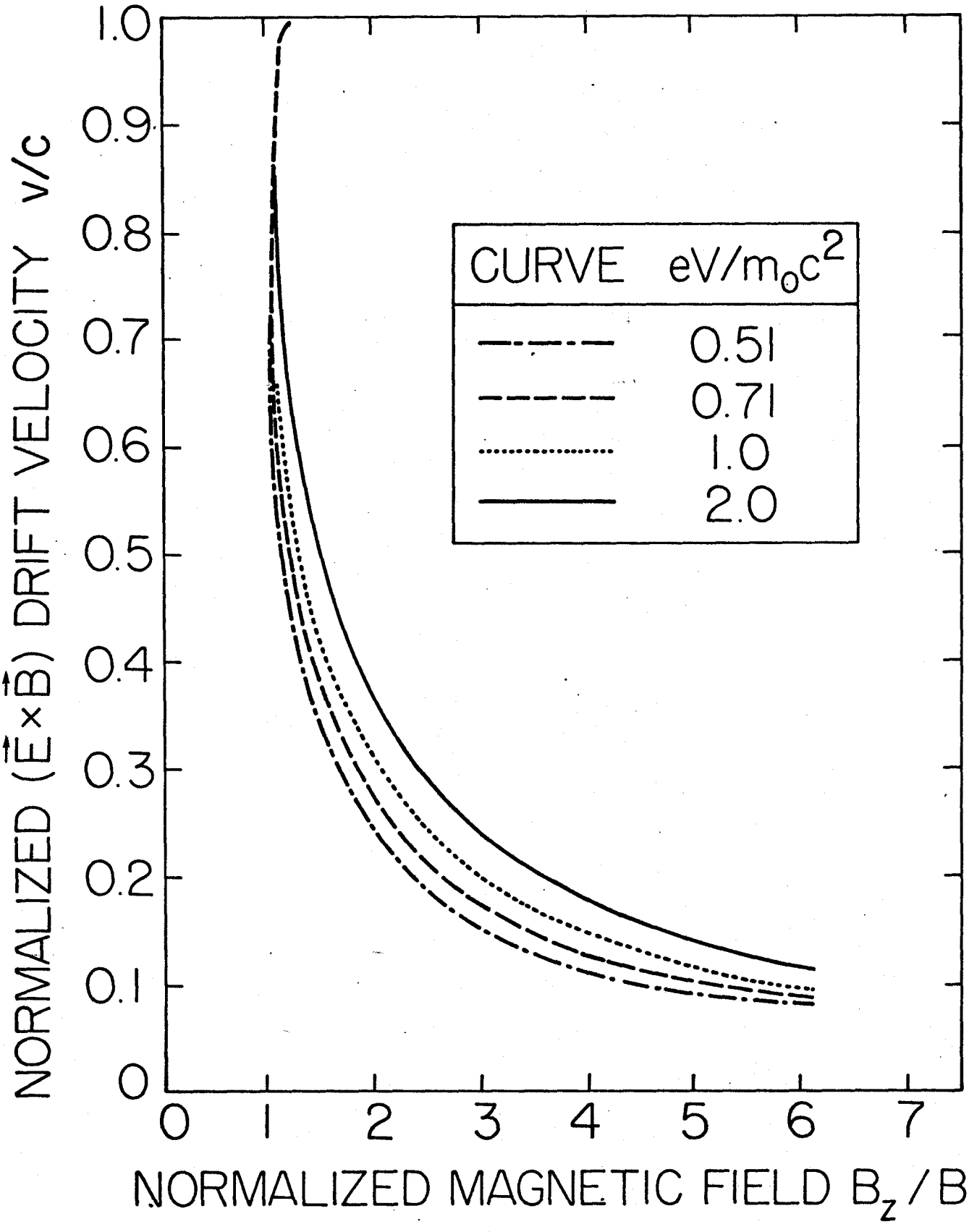

Fig. 5
Orzechowski & Bekefi

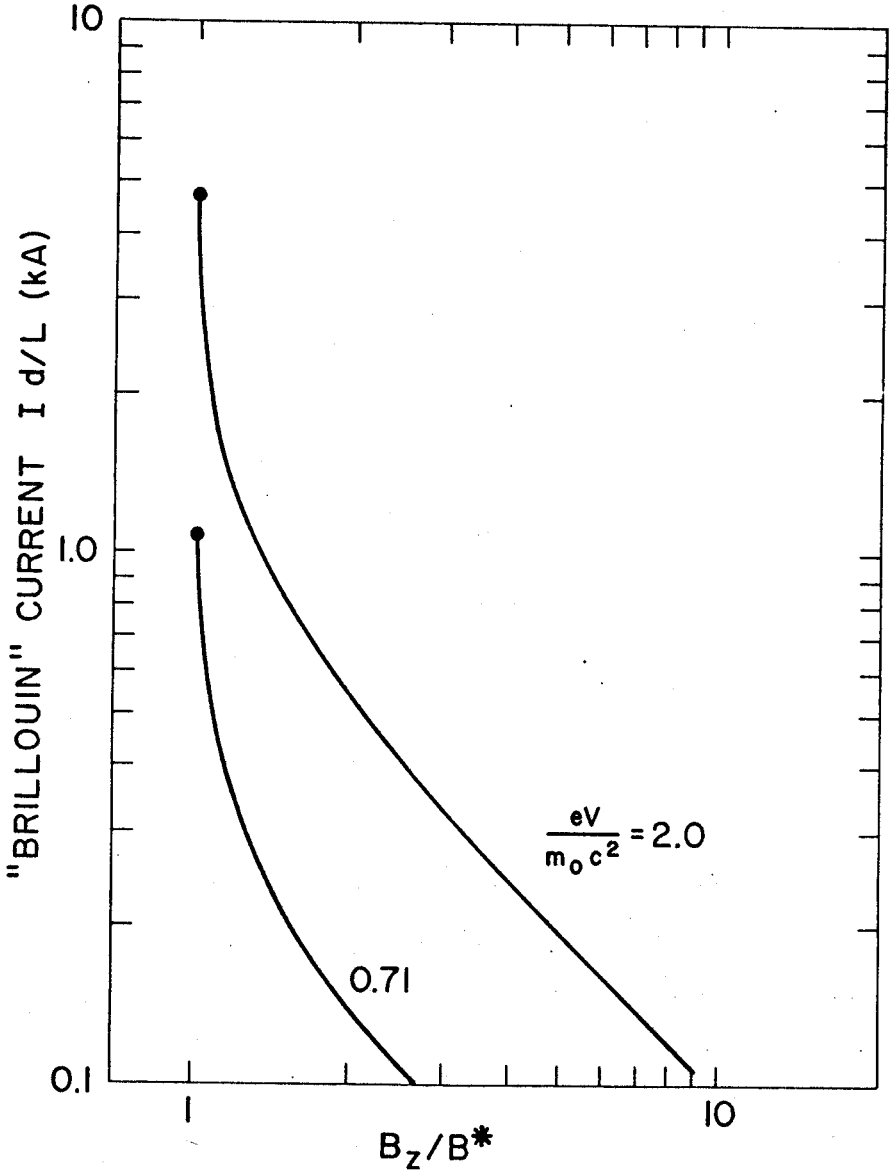

Fig. 6
Orzechowski & Bekefi

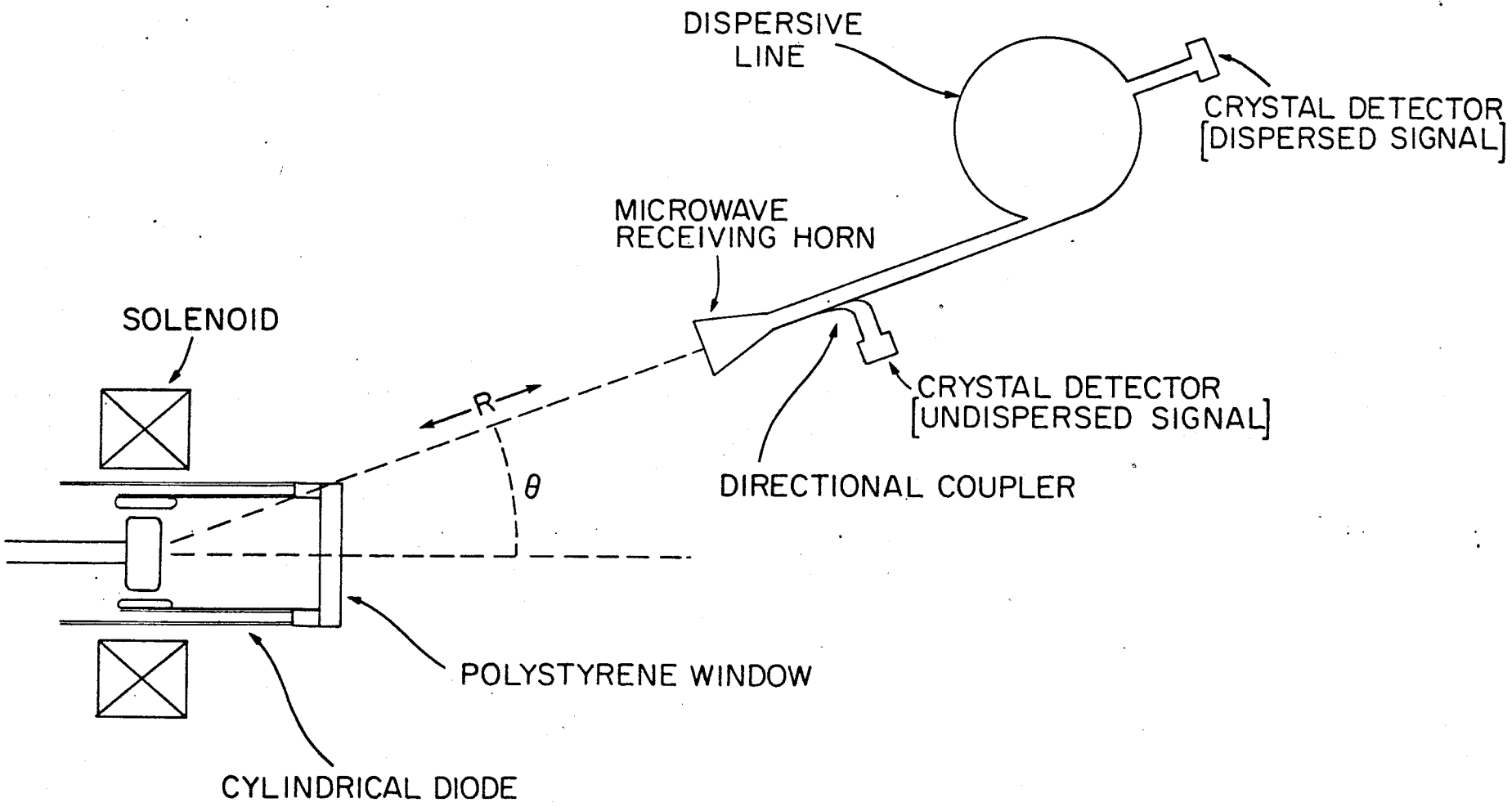

Fig. 7
Orzechowski & Bekefi

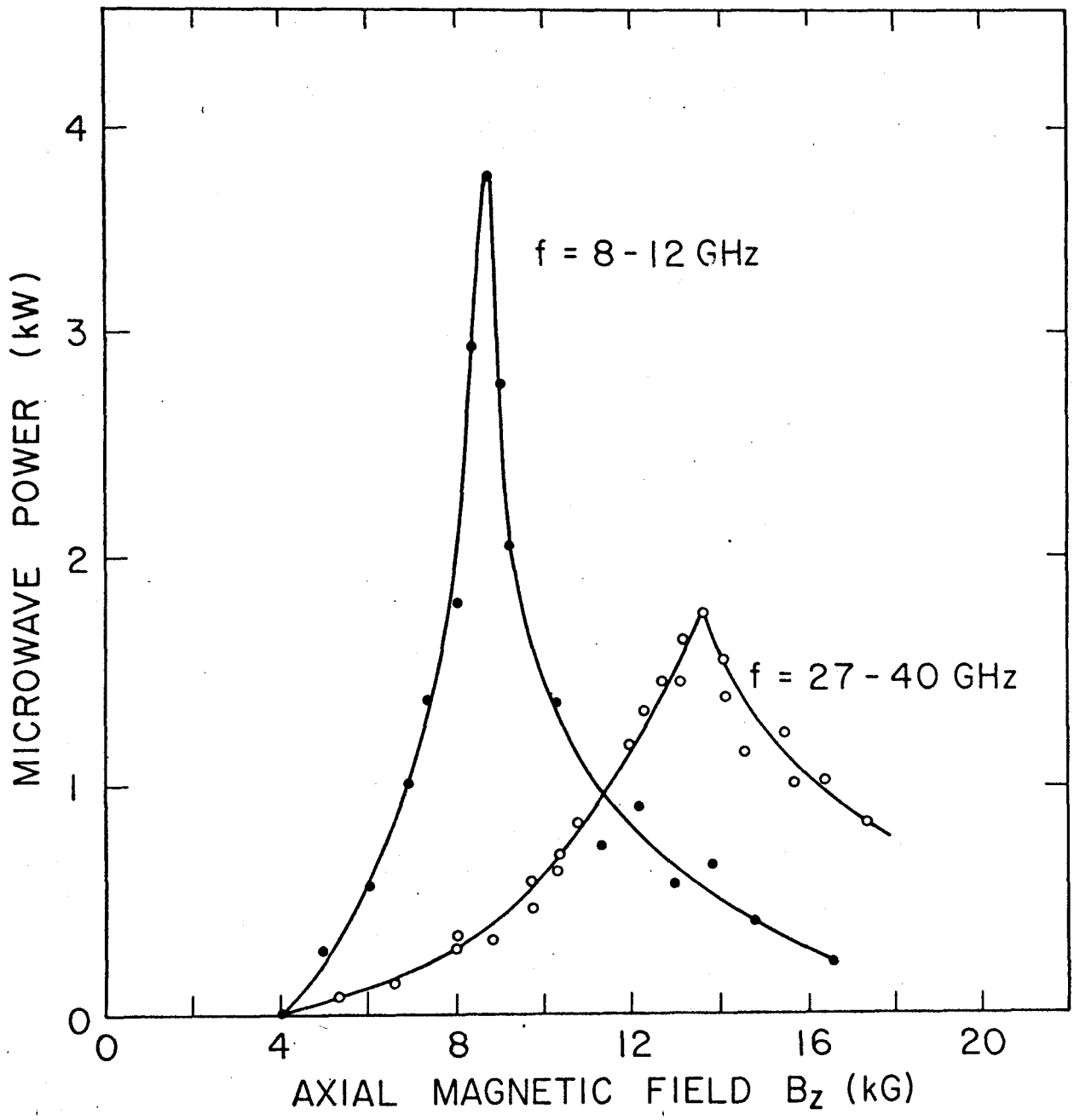

Fig. 8
Orzechowski & Bekefi

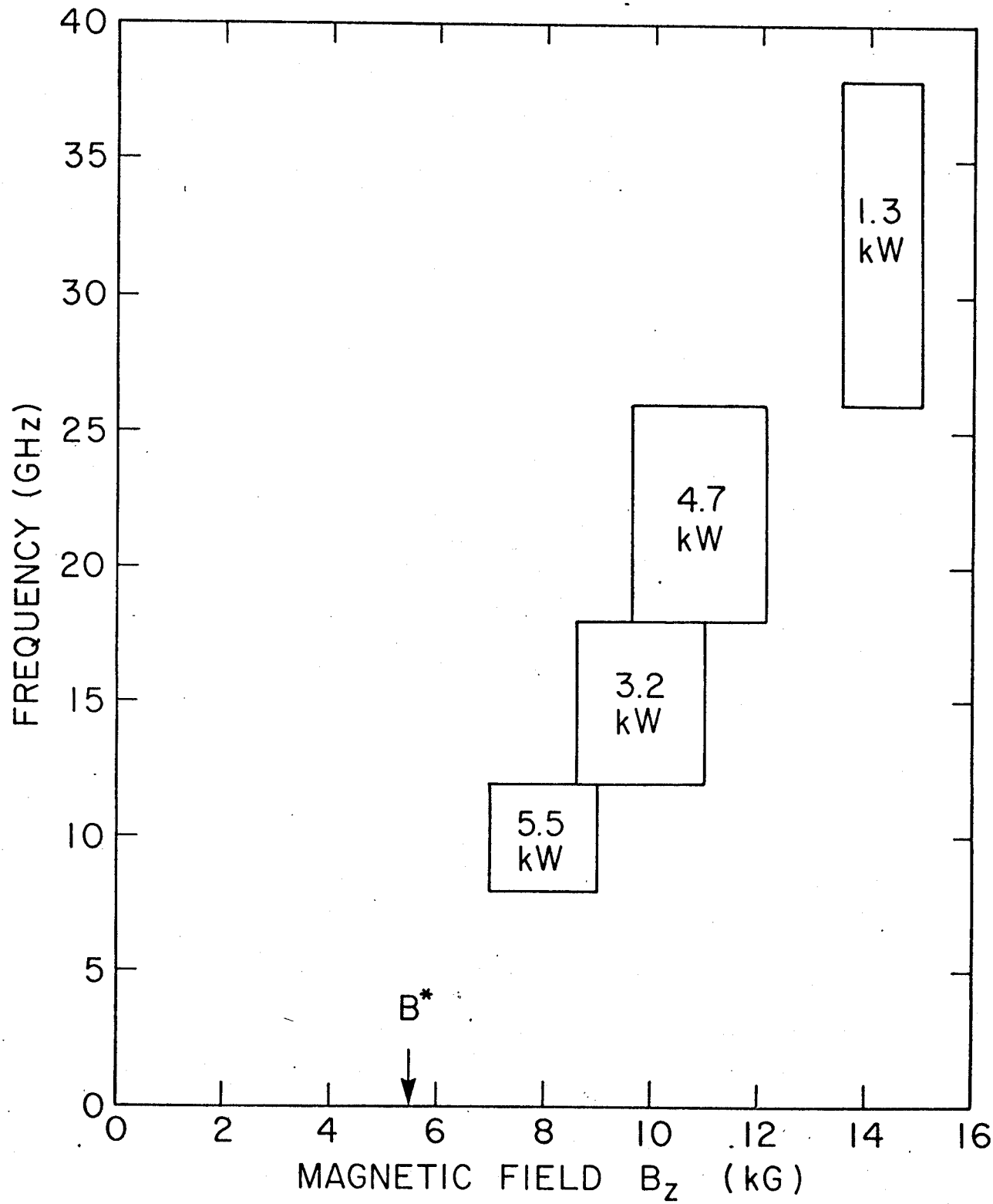

Fig. 9
Orzechowski & Bekefi

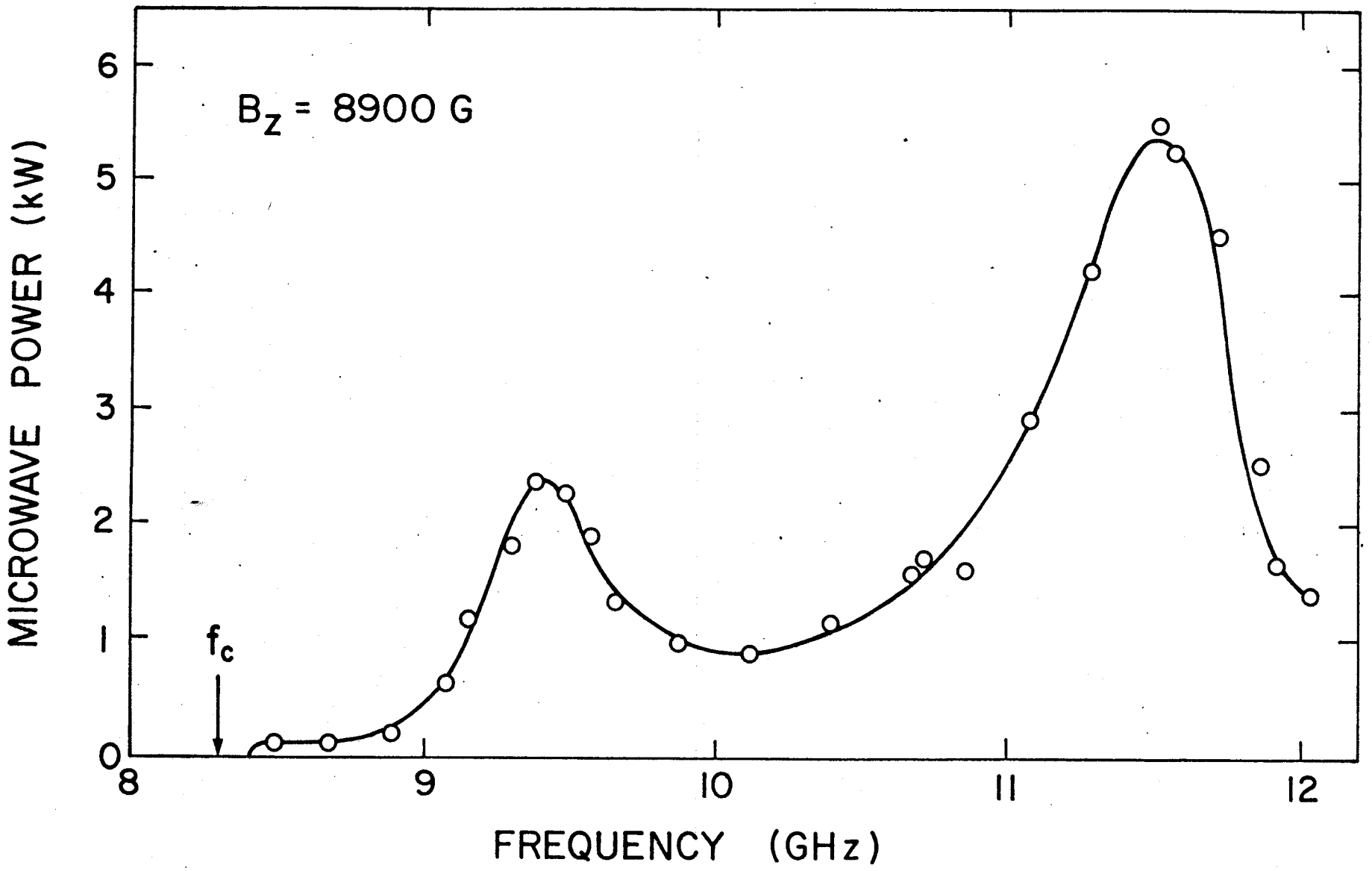

Fig. 10
Orzechowski & Bekefi

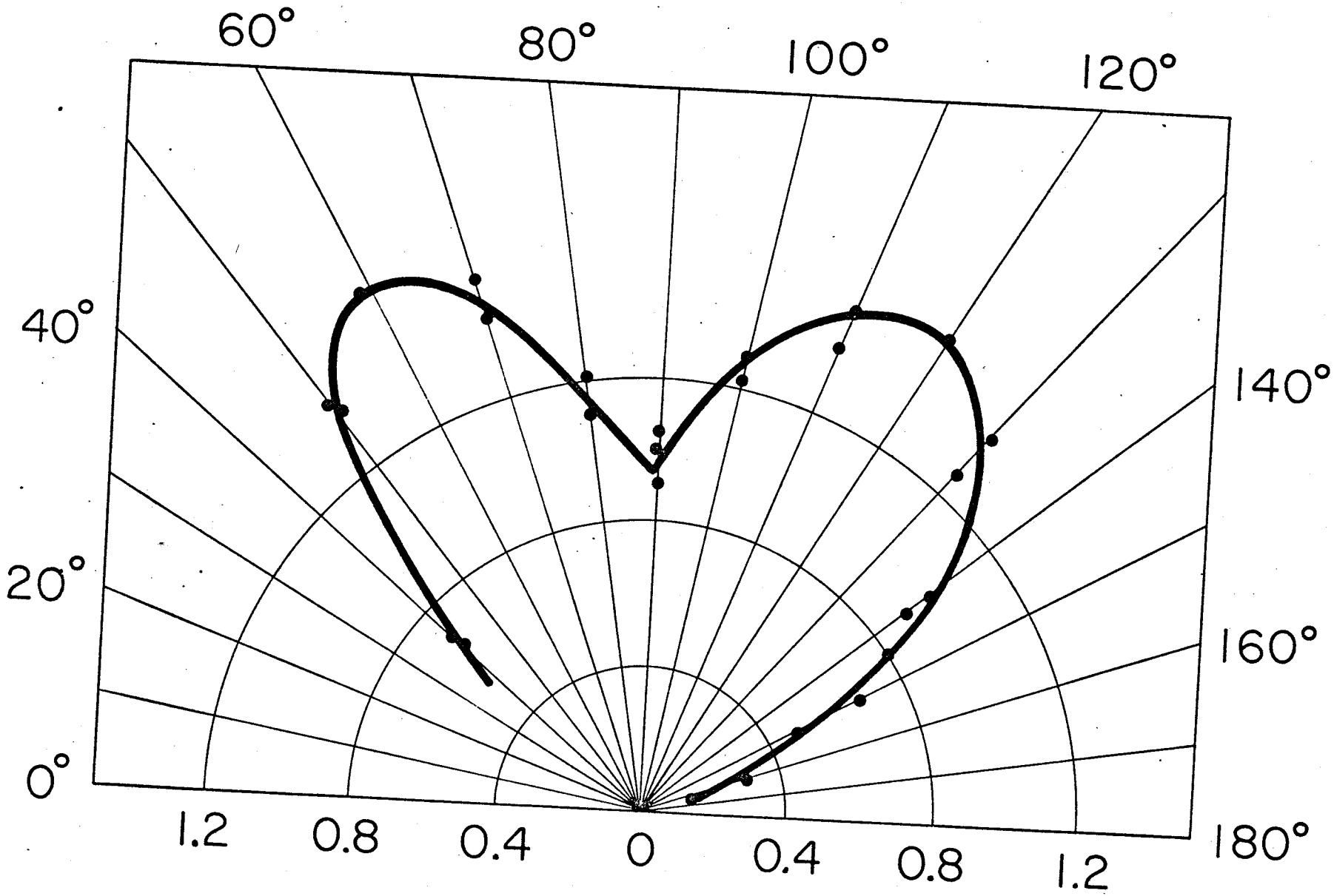

Fig. 11
Orzechowski & Bekefi